Journal of Materials Chemistry A

From Binary to Quaternary: High-tolerance of Multi-acceptors Enables Efficient Polymer Solar Cells

Journal:	*Journal of Materials Chemistry A*
Manuscript ID	TA-ART-01-2019-000948.R1
Article Type:	Paper
Date Submitted by the Author:	23-Feb-2019
Complete List of Authors:	Liu, Longzhu; Southern University of Science and Technology, Chemistry Chen, Hui; Southern University of Science and Technology, Chemistry Chen, Wei; Argonne National Laboratory, Institute for Molecular Engineering and Materials Science Division; University of Chicago, Institute for Molecular Engineering He, Feng; Southern University of Science and Technology, Chemistry

From Binary to Quaternary: High-tolerance of Multi-acceptors Enables Efficient Polymer Solar Cells

Longzhu Liu, [a,b] *Hui Chen,*[a] *Wei Chen,* [c, d] *and Feng He* [a,*]

[a] Department of Chemistry and Shenzhen Grubbs Institute, Southern University of Science and Technology, Shenzhen, 518055, P. R. China

[b] School of chemistry and chemical engineering, Harbin Institute of Technology, Harbin, 150001, P. R. China

[c] Materials Science Division, Argonne National Laboratory, 9700 Cass Avenue, Lemont, Illinois, 60439, United States

[d] Institute for Molecular Engineering, The University of Chicago, 5640 South Ellis Avenue, Chicago, Illinois, 60637, United States

* Corresponding author

E-mail address: hef@sustc.edu.cn (F. H.)

Abstract: To optimum coverage of the optical spectrum and further enhancement of the carrier transport, ternary and even more multi-composition strategies have been universally explored. As $PC_{71}BM$ and $PC_{61}BM$ are both compatible with PTB7-Th, and IEICO-4F takes advantage of optical absorption in the near-infrared region, we combined PTB7-Th:IEICO-4F:$PC_{71}BM$:$PC_{61}BM$ quaternary compositions to fabricate high-efficiency

polymer solar cells (PSCs) with good tolerance ratios of the fullerene acceptors. After blending the fullerene alloy $PC_{71}BM$ and $PC_{61}BM$ into the host PTB7-Th:IEICO-4F system, the optical response in the whole wavelength regime has been strengthened with significantly enhanced electron mobility. Concomitantly, short-circuit current density (*Jsc*) surged from 22.07 to 24.37 mA cm^{-2} and fill factor (FF) ascended from 58.24% to 69.30%, which finally resulted in a champion power conversion efficiency (PCE) of 12.52%, which is much higher than that of the binary control device (9.67%). This significant improvement is attributed to the fine-tuning of the morphology of photo-active layer and feasible carrier transport. Interestingly, this finding implicates the synergistic effect of $PC_{71}BM$ and $PC_{61}BM$ to successfully enhancing the carrier transport. In addition, it demonstrates a broad tolerance of acceptor proportions, resulting in higher PCE for the quaternary devices as compared to ternary devices. Lastly, generality for other systems evidences and provides guidelines for quaternary strategy utilization. Thus, the simplicity of quaternary strategies could be greatly beneficial to not yet elaborate commercial process.

Key words: polymer solar cells, quaternary, high tolerance, carrier transport

Introduction

Polymer solar cells (PSCs) have been prevalently investigated for their obvious advantage of solution processing, low material consumption, and great potential to photovoltaic devices,[1, 2] and stretchable applications.[3, 4] Under this circumstance, crucial standards of devices especially the higher power conversion efficiency (PCE) and easier fabrication were what competed to chase for. Through material innovations and synthesis, many efficient and

popular molecules emerged. For instance PTB7-Th,[5, 6] PBDB-T[7-9], the modified D-A conjugated polymers based on BDT unity as donors paired with various non-fullerene small molecular acceptors including ITIC.[7] . Recent acceptors with distinguished red-shifts achieved notable absorptions in the near-red to infrared regime, such as IEICO-4F and i-IEICO-4F.[10, 11] To further realize outstanding performance of PSCs general methods like thermal treatment and special additives were utilized in most polymer systems.[12-15] Another strategy is the structure improvement based on the bulk heterojunction (BHJ) architecture.[16] Simple methods based on one-step PSCs are widely developed including the multi-composition design[17-19] and interface engineering.[20-23] As an approach to replenish solar light meanwhile keeping the accessibility of process,[24] ternary and even more multi-composition blends have been proven to be simple and highly efficient method to further pump the device achievements.[25] Except for the well-preserved miscibility of components, exciton generation and dissociation, carrier transport and collection were also able to improve the photovoltaic properties of PSCs. Even though the PCE of binary systems was continuously pushed to another peak because the efficient non-fullerene molecules sprung up, the ternary adoption still found an efficient method to utilize the best of fullerene derivatives actively.[25-30] Fullerene derivatives tend to harvest photons in the short wavelength regime. In contrast, non-fullerene molecules dominate in the near-infrared region thus offering more possibilities to maximize the utilization of spectral absorption. Hence, building on the foundation of ternary solar cells, more attempts emerged to utilizing complementary multi-acceptors like quaternary or even more component blends to pursue high-efficiency solar cells.[31-33]

In general, the desirable third or fourth component was able to improve the morphology of blend film and the enhanced crystallinity leading to favorable charge carrier transport in devices. So far, only few non-fullerene acceptors (NFAs) were selected as the multiple components due to the more complex complementarity of respective absorption spectra and modulation of energy levels. Fullerene derivatives with extraordinary solubility and ability of isotropic electron transport like $PC_{61}BM$ and $PC_{71}BM$, suggested the priority in the multi-acceptors option. Herein, the fullerene derivatives $PC_{71}BM$ and $PC_{61}BM$ have similar physical and chemical properties. Therefore, this combination was chosen as sensitizers into the primary PTB7-Th:IEICO-4F blend film. PTB7-Th was considered as the kind of narrow band gap donor, which was compatible with both the fullerene derivatives and specific non-fullerene small molecule IEICO-4F.

When quaternary devices based on PTB7-Th:IEICO-4F:$PC_{71}BM$:$PC_{61}BM$ were fabricated, the excellent isotropic ability to transport electron of fullerene derivatives compensated the anisotropic transport properties of non-fullerene linear conjugated chains. In this work, we mainly worked on quaternary PSCs and achieved the champion device with a PCE of 12.52%, which was about 30% higher than that of its binary control device. Even compared to the highest PCE (11.32%) of ternary devices (PTB7-Th:IEICO-4F:$PC_{71}BM$), the quaternary strategy still increased by 10%. Interestingly, the coordinating effect of $PC_{71}BM$ and $PC_{61}BM$ cooperation not only revealed an enhanced carrier transport compared to the binary system. It also showed high PCEs all around about 12% in a relatively big region of added $PC_{71}BM$ and $PC_{61}BM$. Finally, we applied this strategy to other systems based on PTB7-Th:NFAs:$PC_{71}BM$:$PC_{61}BM$, where NFAs represented the respective ITIC, IT-M,

IT-4F. The present results demonstrate the generality of synergistic effects of $PC_{71}BM$ and $PC_{61}BM$ thus enabling high-efficiency quaternary devices. The present work is expected to provide a broader choice for PSCs to industrial production.

Results and Discussion

2.1 Chemical structures and energy levels

The chemical structures of used components are shown in Figure 1. PTB7-Th is a classical conjugated polymer donor with narrow band gap, which was widely used to match with various fullerene derivatives. The non-fullerene acceptor IEICO-4F is designed as A-D-A-type small molecule, which possesses a narrow band gap via the introduced alkoxy and fluorine atoms. Although $PC_{71}BM$ and $PC_{61}BM$ have similar structure, the larger size and shape of $PC_{71}BM$ differentiate with each other. The energy levels of the materials are presented in Figure 1e. The fullerene derivatives have energetically aligned LUMOs that may offer a tendency to form alloy structures[34,35] upon addition into the binary host. The induced energy levels match well thus a cascade was formatted between PTB7-Th:IEICO-4F, which is beneficial for high-efficiency charge separation and charge transfer.[36] In Figure 1f, the optical absorption of the host PTB7-Th and IEICO-4F neat film peaked at about 700 nm and 900 nm, respectively. In contrast, the $PC_{61}BM$ absorption is mainly located in violet region with weak extension into the visible region and $PC_{71}BM$ films mainly harvested light in the regime from 300 - 500 nm. Thus, the combination of $PC_{71}BM$:$PC_{61}BM$ was supposed as helpful component easily avoiding excessive spectral overlap and complementarily covering the comprehensive spectrum.

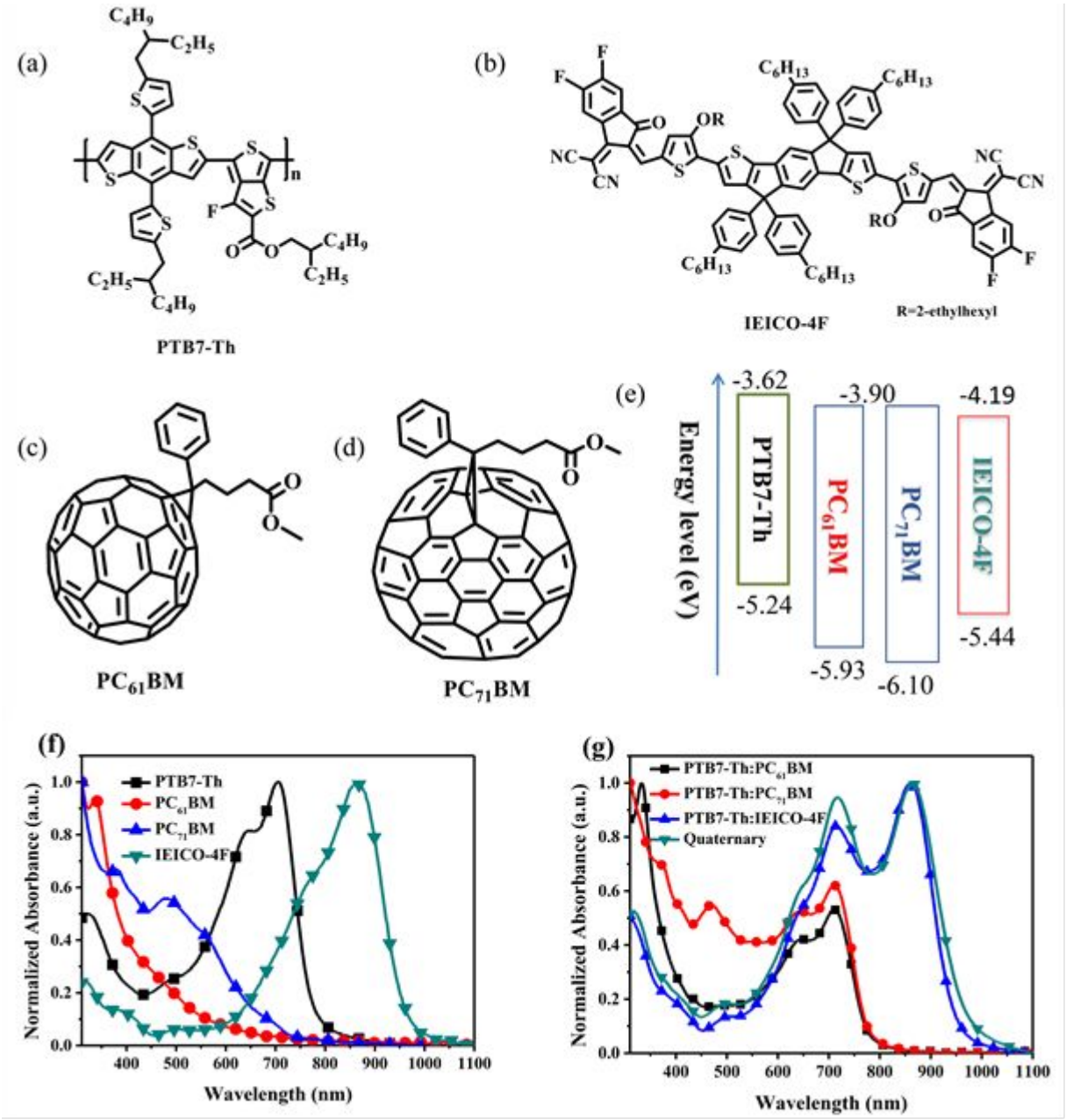

Figure 1. Chemical structures of (a) PTB7-Th, (b) IEICO-4F, (c) $PC_{61}BM$, (d) $PC_{71}BM$; (e) Energy levels of PTB7-Th, $PC_{61}BM$, $PC_{71}BM$, IEICO-4F. UV-vis absorption of (f) neat and (g) blend films.

2.2 Photovoltaic performance

Table 1. The performance parameters of PSCs based on binary and quaternary devices under 100 mW cm^{-2} AM 1.5 G irradiation.

Composition	*Voc* (V)	*Jsc* (mA cm^{-2})	FF (%)	PCE (%)	*Jcal*[a]
PTB7-Th:$PC_{61}BM$	0.81	14.79	65.28	7.86 (7.66±0.20)[b]	14.42
PTB7-Th:$PC_{71}BM$	0.80	15.74	69.20	8.74 (8.50±0.24)	15.51
PTB7-Th:IEICO-4F	0.75	22.06	58.24	9.67 (9.50±0.17)	21.35
PTB7-Th:IEICO-4F:$PC_{71}BM$[c]	0.75	23.17	65.03	11.32 (11.06±0.26)	22.51
Quaternary	**0.74**	**24.37**	**69.30**	**12.52 (12.31±0.22)**	**23.78**

[a] The calculated *Jsc* values from EQE curves;
[b] Average value ± standard deviation were calculated from the statistics of 20 different devices
[c] best values of best ternary devices.

Detailed data about the performance of PSCs based on binary and quaternary (PTB7-Th:IEICO-4F:$PC_{71}BM$:$PC_{61}BM$) devices were summarized in Table 1. Obviously, the binary fullerene devices took advantage in a high FF of over 65%, but the values of *Jsc* were moderate. In contrast, PTB7-Th:IEICO-4F devices were just going the opposite tendency (high *Jsc* of 22.07 mA cm^{-2}, low FF of 58.24%, PCE of 9.67%). From the binary to quaternary devices, the booming performance is mainly attributed to the increased *Jsc* of 24.37 mA cm^{-2} and surged FF of 69.30%, which finally resulted in a champion PCE of 12.52%. Concerning further details, the best performance derived from PTB7-Th:IEICO-4F:$PC_{71}BM$:$PC_{61}BM$ devices were achieved at optimized proportion of 1:1.1:0.2:0.2 (*w*/*w*). Other devices including binary, ternary, and quaternary were fixed at

D/A (total ratio) =1:1.5 ratios. Also, the performance of ternary devices with varying proportions of either $PC_{71}BM$ or $PC_{61}BM$ (Table S1 and Figure S1) more clearly exhibited a gradual increase in *Jsc* and FF as a bridge connecting the binary and quaternary devices. As shown in Table S1, the optimized ternary devices showed a PCE of 11.32% (with $PC_{71}BM$ added only), and 11.13% (with $PC_{61}BM$ added only), respectively. The ternary PSCs with $PC_{61}BM$ caused smaller series resistance (Rs) than that of $PC_{71}BM$ based ternary devices, producing the high FF in devices. In return, the main contribution from $PC_{71}BM$ in ternary devices was the significantly enhanced *Jsc*. When combining the merits of $PC_{61}BM$ and $PC_{71}BM$, the expected quaternary devices have the improved *Jsc* and FF, generating a PCE in the respective quaternary devices beyond 12% under the high tolerance ratios of fullerene components (Table S1 and Figure S2).

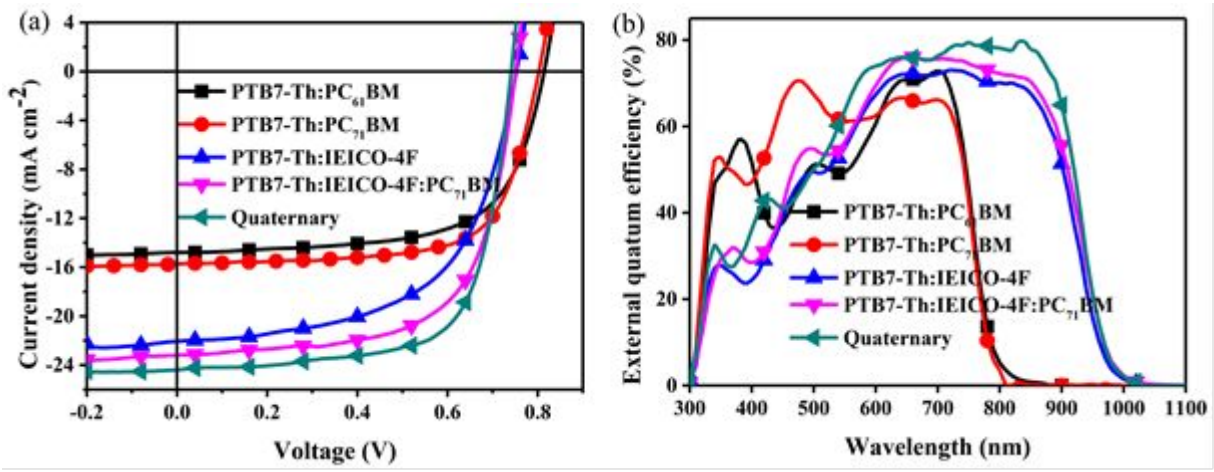

Figure 2. (a) J-V and (b) EQE curves of PSCs based on binary (PTB7-Th:$PC_{61}BM$, PTB7-Th:$PC_{71}BM$, PTB7-Th:IEICO-4F) , the best ternary and quaternary devices under 100 mW cm^{-2} AM 1.5 G irradiation.

To explore the reasons of increased *Jsc* in the quaternary devices, the external quantum efficiency (EQE) spectra of all devices were measured in the wavelength range from 300 to

1100 nm. From the EQE spectrum, the PTB7-Th:IEICO-4F device was fully elevated to higher level rather than certain specific region, which could correspond to more intensive light response in quaternary devices (Figure 2b). Especially, the notable response values were maintaining about 80% from 700 to 900 nm for the quaternary devices. This seems to be the prominent contribution for the enhanced *Jsc* (Figure 2a). $PC_{71}BM$ and $PC_{61}BM$ were nearly without absorption in this wavelength region, but both of them showed favorable electron mobility. Incorporating them into PTB7-Th:IEICO-4F, the newly formed quaternary devices qualified for better exciton separation and charge transport. As expected, the quaternary devices obtained the high EQE values in the whole response area.

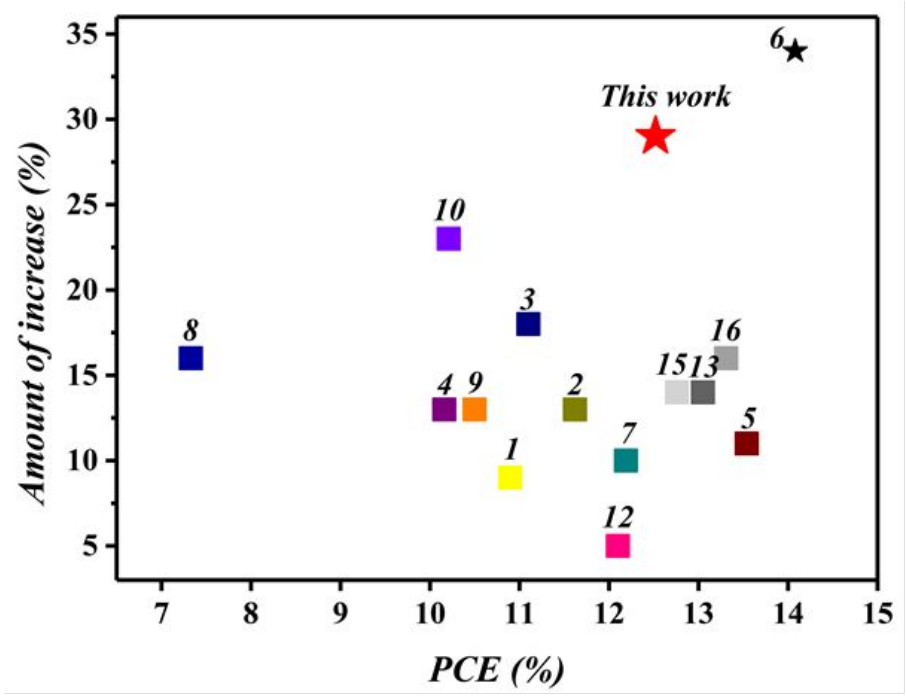

Figure 3. The summary of amount of increase referring recent ternary and even more multi-components systems, where the number was presented to the corresponding reference in supporting information.

To evaluate our study on the whole, we summarized a series of relevant references and skeletonized their performances in Figure 3 and Table S5. Although the result presented in

this work does not stand on the top of this research field (red star in Figure 3) it demonstrates that the performances of quaternary device increases by about 30% compared to the binary control devices. The highest increase is about 34% in a ternary device compared to its binary device, marked as black star in the Figure 3The results indicate that the quaternary strategy is competitive to ternary or other multi-components methods to further pump the PCE in IEICO-4F-based system.

2.3 Film Morphology

The performance of PSCs is closely correlated the blend morphology, phase aggregation, and molecular orientation in the photo-active layer.[27, 37-39] To better understand the relationship between the morphology and performance when going from binary to quaternary devices, we utilized atomic force microscopy (AFM) and transmission electron microscopy (TEM) to characterize the morphology change. The AFM and TEM images of different components are displayed in Figure S3. The binary PTB7-Th:IEICO-4F film exhibits the smallest root-mean-square (RMS) roughness of 1.15 nm, and a similar surface roughness of 1.30 nm was acquired in PTB7-Th:$PC_{61}BM$ and PTB7-Th:$PC_{71}BM$ films. For the quaternary compositions, the surface RMS value (2.31 nm) was about twice as high as that of PTB7-Th:IEICO-4F. The TEM images implied more apparent aggregations in fullerene-containing binary films In contrast, because of the good planar conjugated structure and high steric hindrance of IEICO-4F, the PTB7-Th:IEICO-4F films tended to be amorphous as shown in Figure S3g. So when the $PC_{71}BM$ and $PC_{61}BM$ joined the PTB7-Th:IEICO-4F film (Figure S3h), the quaternary blend built up a more suitable

nanoscale interpenetrating network. In addition, the phase separation exhibited a more moderate aggregation in favor of the exciton dissociation.

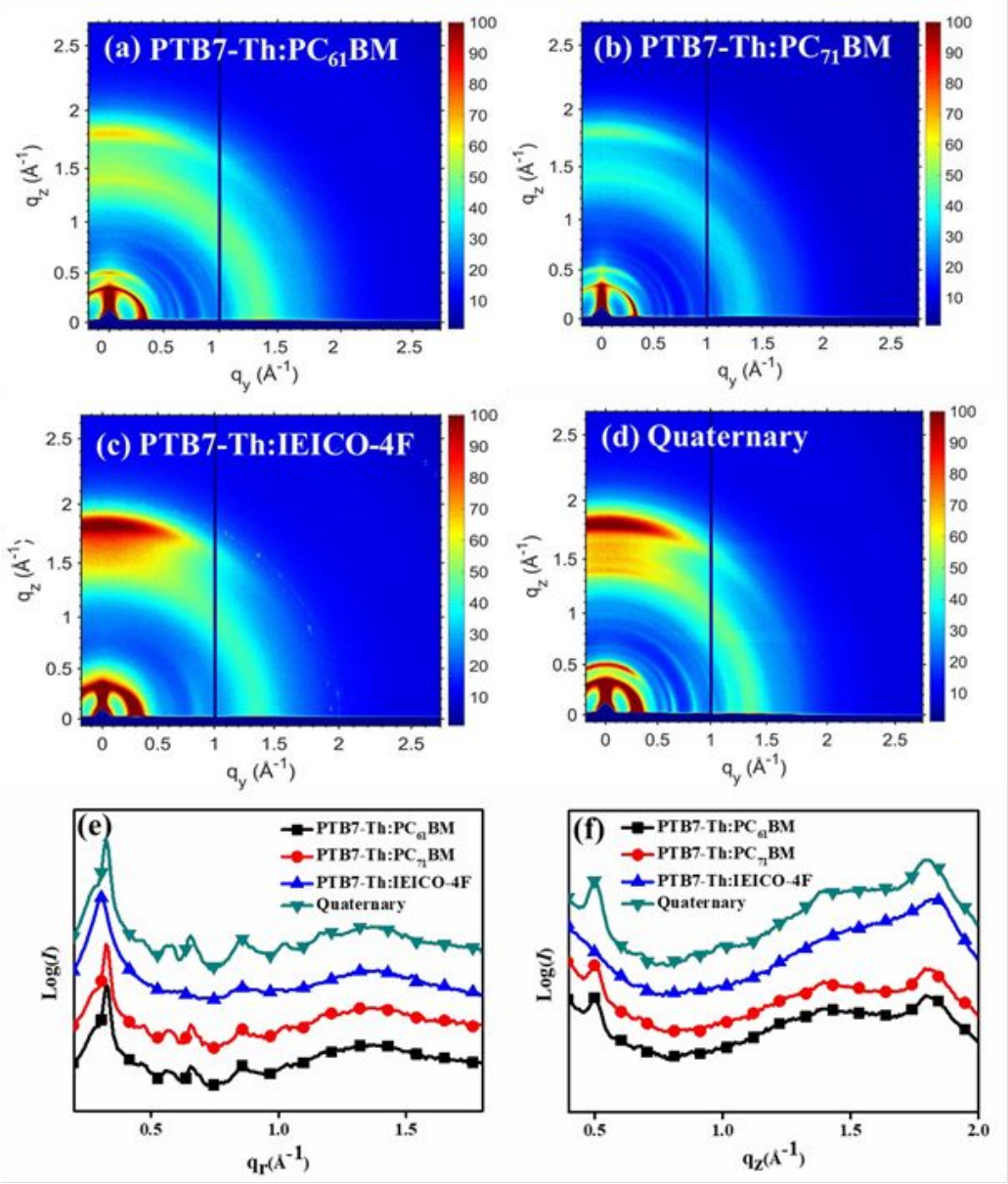

Figure 4. GIWAXS patterns of (a) PTB7-Th:$PC_{61}BM$, (b) PTB7-Th:$PC_{71}BM$, (c) PTB7-Th:IEICO-4F and (d) quaternary; (e) out-of-plane and (f) in-plane linecut profiles based on binary (PTB7-Th:$PC_{61}BM$, PTB7-Th:$PC_{71}BM$, PTB7-Th:IEICO-4F) and quaternary blend films.

To obtain detailed information on blend films, the grazing incident wide-angle X-ray scattering (GIWAXS) was utilized to explore the crystallinity and the molecular packing. Figures 4a to 4d display 2D GIWAXS patterns for various blend films. The corresponding

line cuts for the out-of-plane and in-plane profiles are plotted in Figures 4e and 4f, respectively. From the out-of-plane profiles, we find the characteristic π-π stacking peaks around 1.80 $Å^{-1}$ corresponding π-π distances about 3.49 Å implying a prominent "face-on" feature in all blend films. However, the different blend films show some discrepancies around 0.30 $Å^{-1}$ in the in-plane profiles. Although the films possessed the obvious lamellar stacking, the calculated full width at half maximum (FWHM) of different components films changed upon incorporation of the fullerene. The FWHM of host PTB7-Th:IEICO-4F has the largest value of 0.11 $Å^{-1}$, indicating smallest coherence length of 4.95 nm on the basis of the Scherrer equation[40, 41]. The FWHM of two fullerene blend films had the small value of about 0.05 $Å^{-1}$, indicating coherence length about 11.78 nm. For the optimal quaternary blend film, the FWHM values to 0.08 $Å^{-1}$ corresponding to a coherence length was 6.82 nm. Considering that a larger coherence length affirms a positive impact[40, 42] on the quaternary device in the presence of $PC_{71}BM$:$PC_{61}BM$, we conclude on a more efficient exciton separation and carrier transport resulting in the enhancement of *Jsc* and FF. The mobilities derived from space-charge-limited current (SCLC) (Table S2 and Figure S4) also support the above description. The electron mobility (μ_h) and hole mobility (μ_e) of PTB7-Th:$PC_{61}BM$, PTB7-Th:$PC_{71}BM$ revealed subtle differences, whereas the PTB7-Th:IEICO-4F and quaternary showed relatively big variation. The μ_h and μ_e values of quaternary devices approached the highest values around 9.3×10^{-4} and 1.0×10^{-3} ($cm^2\ V^{-1}\ S^{-1}$) and balanced μ_h/μ_e value compared to other three devices, evidently displaying the superior charge transport. On the other hand, high and balanced carrier mobility could decline the charge accumulation and

built-in electric field erosion so that the *Jsc* and FF of quaternary devices would reach the values of expectation.

2.4 Carrier transport

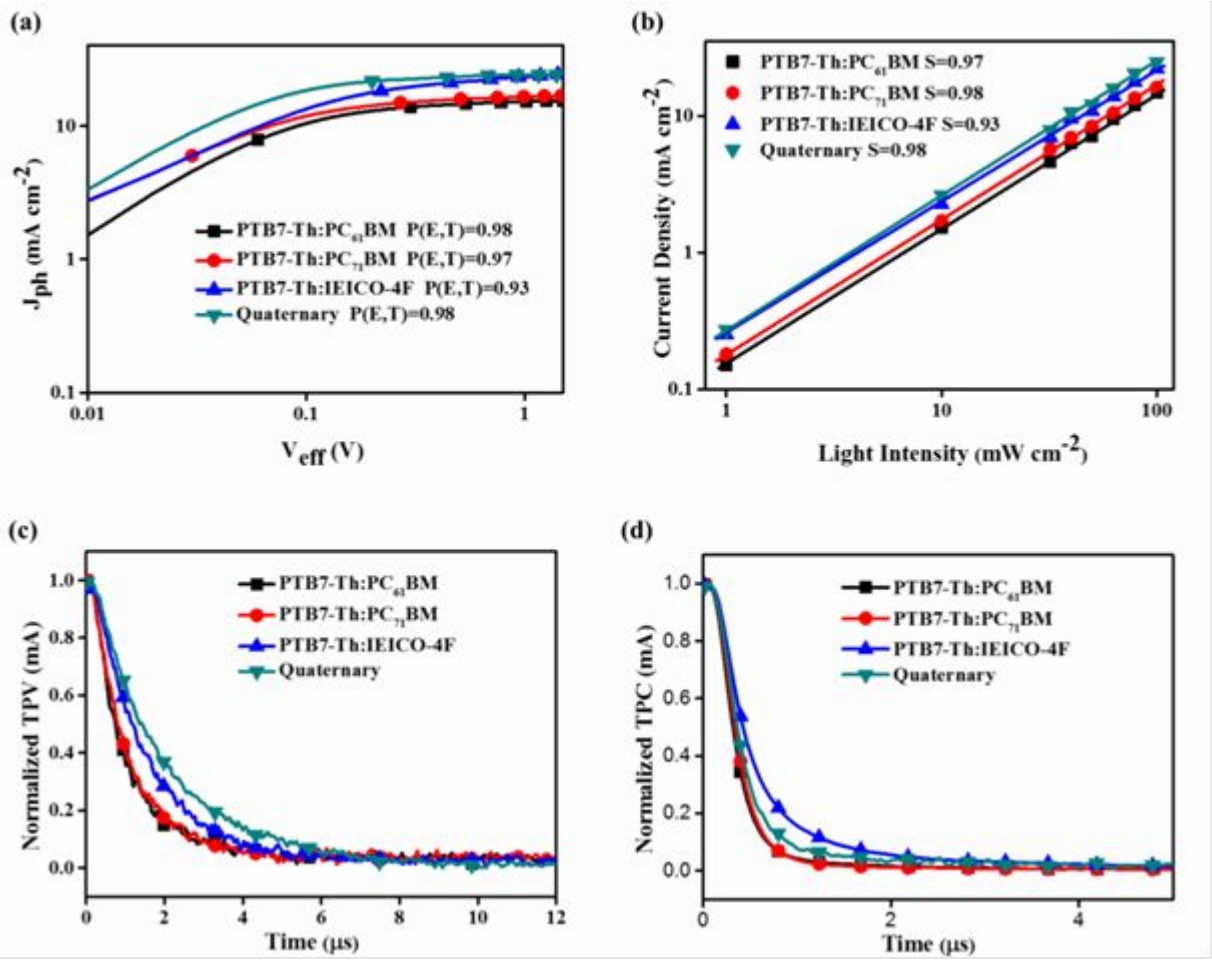

Figure 5. (a) Jph-Veff curves; (b) Light intensity dependence fitting lines (c) Transient photovoltage and (d) transient photocurrent measurements based on binary (PTB7-Th:PC_{61}BM, PTB7-Th:PC_{71}BM,PTB7-Th:IEICO-4F) and quaternary devices.

As known, the morphology could affect the exciton dissociation and charge transport. To better understand the exciton dissociation process when going from the binary to quaternary device, the exciton dissociation probabilities (P(E,T) = Jph/Jsat) were measured (Figure 5a). The binary fullerene devices had the high P(E,T) above 0.97, indicating that the

excitons in PTB7-Th:$PC_{61}BM$ and PTB7-Th:$PC_{71}BM$ quickly dissociated into free carriers thus quickly achieving the saturation regime. The P(E,T) of PTB7-Th:IEICO-4F IEICO-4F was only 0.93, but the combined quaternary device maintained the merit of binary fullerene devices with P(E,T) up to 0.98 leading to improved exciton dissociation. To get further insight the carrier recombination was measured by *Jsc* versus light-intensity (Plight) as dependent on a function of $Jsc \propto Plight^{\alpha}$, (Figure 5b). The slope of quaternary devices considerably raised to 0.98 compared to PTB7-Th:IEICO-4F (α=0.93) based devices. Obviously, the suppressed bimolecular recombination should be attributed to the $PC_{71}BM$:$PC_{61}BM$ addition for the similar refrained recombination in PTB7-Th:$PC_{61}BM$ (α=0.97) and PTB7-Th:$PC_{71}BM$ (α=0.98). Thus, with generating dissociated excitons more efficiently and restrained more loss of charge recombination, this lays a solid foundation of later carrier extraction thereby comprehend better upward *Jsc* and FF in quaternary based devices.

Subsequently, to verify a deep understanding of the device under operation conditions, the transient photovoltage (TPV) and transient photocurrent (TPC) measurements were explored (see Figures 5c and 5d). The extracted data are summarized in Table S3. From the fitted TPC curves (Figure 5d), the calculated times of charge extraction (t_s) was 0.22, 0.23, 0.34, 0.26 μs for the devices based on PTB7-Th:$PC_{61}BM$, PTB7-Th:$PC_{71}BM$, PTB7-Th:IEICO-4F and quaternary devices, respectively. Concurrently, the carrier lifetime (τ_R) from TPV test (Figure 5c) under open circuit condition was analyzed as 0.65, 0.70, 0.96, 1.21 μs for the same device sequence (PTB7-Th:$PC_{61}BM$, PTB7-Th:$PC_{71}BM$, PTB7-Th:IEICO-4F and quaternary)We may suspect that the PTB7-Th:IEICO-4F blend has a

higher photo-generated quantum yield among the investigated binary systems due to its higher light response[43]. Evidently, the integration of enlarged carrier lifetime and fastest collection to electrodes supports that quaternary devices perform the best carrier transport behavior. In addition, it could be roughly inferred that carrier diffusion length $\propto \mu \tau_R$ (where μ represents the mobility as discussed above),[44-47] The enhanced carrier diffusion length is thus able to increase the valid charge transport in the more efficient devices.

2.5 Generality

To explore the wider application of quaternary strategies, we fabricated other quaternary devices with other NFAs systems. Therein, we choose the popular NFAs such as ITIC, IT-M and IT-4F, respectively. Detailed performance parameters of different quaternary PSCs in comparison with their corresponding binary devices are listed in Table S4. Like the quaternary systems based on IEICO-4F, the other systems only tolerated a negligible loss of *Voc*, which is attributed the gap between the HOMO value of the donors and the lowest LUMO from NFAs, too.[27, 48] Overall, the synergistic effects of balanced $PC_{71}BM$:$PC_{61}BM$ impacted positively on the different host binary compositions mainly resulting from the improvement of *Jsc*. It is worth to note that the PSCs based on PTB7-Th:IT-4F:0.2$PC_{71}BM$:0.2$PC_{61}BM$ device showed considerable FF of 71.27% and *Jsc* of 18.59 mA cm^{-2} increasing by almost 15% in PCE compared to binary pristine IT-4F based devices.,This agrees well with the results of the PTB7-Th:IEICO-4F:$PC_{71}BM$:$PC_{61}BM$ devices. In addition, we found the light response from the EQE spectrum to become stronger with the change of ITIC, IT-M and IT-4F (see Figures S5-S7). Most importantly, it is promising as a general and efficient method for promoting the performance of those NFAs

systems suffering from the inferior carrier transport by optimized quaternary components in blend films.

Conclusions

In summary, the photovoltaic performance of champion quaternary (PTB7-Th:IEICO-4F:$PC_{71}BM$:$PC_{61}BM$=1:1.1:0.2:0.2) devices achieved a PCE of 12.52% due to both, the device current density J_{SC} and the fill factor *FF*. Upon $PC_{71}BM$:$PC_{61}BM$ additions to PTB7-Th:IEICO-4F binary blends, the quaternary devices combined the merits of high FF from PTB7-Th:$PC_{71}BM$ or $PC_{61}BM$ and high *Jsc* from PTB7-Th:IEICO-4F. Addition of the fullerenes induces fine-tuning of the morphology of these triple acceptors and higher degree of structural order in the molecular packing. The quaternary systems are found to form better interpenetrating networks, enhancing the exciton dissociation and the carrier transport. Moreover, because the *Voc* of the quaternary devices is adhered to that of devices based on PTB7-Th:IEICO-4F. Enhanced carrier transport and suppressive recombination could easily explain effects that would embody at considerably improved *Jsc* and FF in comparison. Although the complexity of device compositions slightly increased, our study on quaternary PSCs could offer more references to collocate and develop photovoltaic materials for high-efficiency polymer-based solar cells.

Conflict of interest

The authors declare no competing financial interests.

Acknowledgements

This work was financially supported by the National Natural Science Foundation of China (51773087, 21733005), the Shenzhen Fundamental Research program (JCYJ20170817111214740) and the Shenzhen Nobel Prize Scientists Laboratory Project (C17783101). W. C. gratefully acknowledges financial support from the US Department of Energy, Office of Science, Materials Science and Engineering Division. We also thank Dr. Joseph Strzalka and Dr. Zhang Jiang for their assistance with GIWAXS measurements. Use of the Advanced Photon Source (APS) at the Argonne National Laboratory was supported by the U.S. Department of Energy, Office of Science, Office of Basic Energy Sciences under contract no. DE-AC02-06CH11357.

References

1. W. Wang, C. Yan, T. K. Lau, J. Wang, K. Liu, Y. Fan, X. Lu and X. Zhan, *Adv. Mater.*, 2017, **29**,1701308.
2. Y.-W. Su, S.-C. Lan and K.-H. Wei, *Mater. Today*, 2012, **15**, 554-562.
3. S. Pan, Z. Yang, P. Chen, J. Deng, H. Li and H. Peng, *Angew. Chem., Int. Ed.,* 2014, **53**, 6110-6114.
4. H. Jinno, K. Fukuda, X. Xu, S. Park, Y. Suzuki, M. Koizumi, T. Yokota, I. Osaka, K. Takimiya and T. Someya, *Nat. Energy*, 2017, **2**, 780-785.
5. S.-H. Liao, H.-J. Jhuo, Y.-S. Cheng and S.-A. Chen, *Adv. Mater.*, 2013, **25**, 4766-4771.
6. S. Zhang, L. Ye, W. Zhao, D. Liu, H. Yao and J. Hou, *Macromolecules*, 2014, **47**, 4653-4659.
7. W. Zhao, D. Qian, S. Zhang, S. Li, O. Inganas, F. Gao and J. Hou, *Adv. Mater.*, 2016, **28**, 4734-4739.

8. W. Zhao, S. Li, H. Yao, S. Zhang, Y. Zhang, B. Yang and J. Hou, *J. Am. Chem. Soc.,* 2017, **139**, 7148-7151.

9. S. Zhang, Y. Qin, J. Zhu and J. Hou, *Adv. Mater.*, 2018, **30**,1800868.

10. H. Yao, Y. Cui, R. Yu, B. Gao, H. Zhang and J. Hou, *Angew. Chem., Int. Ed.,* 2017, **56**, 3045-3049.

11. W. Wang, B. Zhao, Z. Cong, Y. Xie, H. Wu, Q. Liang, S. Liu, F. Liu, C. Gao, H. Wu and Y. Cao, *ACS Energy Lett.,* 2018, **3**, 1499-1507.

12. X. Song, N. Gasparini, L. Ye, H. Yao, J. Hou, H. Ade and D. Baran, *ACS Energy Lett.*, 2018, **3**, 669-676.

13. W. Li, M. Chen, J. Cai, E. L. K. Spooner, H. Zhang, R. S. Gurney, D. Liu, Z. Xiao, D. G. Lidzey, L. Ding and T. Wang, *Joule*, 2018, DOI: 10.1016/j.joule.2018.11.023.

14. C.-M. Liu, Y.-W. Su, J.-M. Jiang, H.-C. Chen, S.-W. Lin, C.-J. Su, U. S. Jeng and K.-H. Wei, *J. Mater. Chem. A*, 2014, **2**, 20760-20769.

15. M. S. Su, C. Y. Kuo, M. C. Yuan, U. S. Jeng, C. J. Su and K. H. Wei, *Adv. Mater*, 2011, **23**, 3315-3319.

16. A. J. Heeger, *Adv. Mater.,* 2014, **26**, 10-27.

17. L. Lu, T. Xu, W. Chen, E. S. Landry and L. Yu, *Nat. Photonics*, 2014, **8**, 716-722.

18. L. Lu, W. Chen, T. Xu and L. Yu, *Nat. Commun.*, 2015, **6**, 7327.

19. X. Ma, Y. Mi, F. Zhang, Q. An, M. Zhang, Z. Hu, X. Liu, J. Zhang and W. Tang, *Adv. Energy Mater.,* 2018, **8**,1702854.

20. H.-L. Yip, S. K. Hau, N. S. Baek, H. Ma and A. K. Y. Jen, *Adv. Mater.*, 2008, **20**, 2376-2382.

21. H. Zhou, Y. Zhang, J. Seifter, S. D. Collins, C. Luo, G. C. Bazan, T. Q. Nguyen and A. J. Heeger, *Adv. Mater.*, 2013, **25**, 1646-1652.

22. Z. Yin, J. Wei and Q. Zheng, *Adv. Sci. (Weinh)*, 2016, **3**, 1500362.

23. Z. Zheng, R. Wang, H. Yao, S. Xie, Y. Zhang, J. Hou, H. Zhou and Z. Tang, *Nano Energy*, 2018, **50**, 169-175.

24. D. Baran, R. S. Ashraf, D. A. Hanifi, M. Abdelsamie, N. Gasparini, J. A. Rohr, S. Holliday, A. Wadsworth, S. Lockett, M. Neophytou, C. J. Emmott, J. Nelson, C. J. Brabec, A. Amassian, A. Salleo, T. Kirchartz, J. R. Durrant and I. McCulloch, *Nat. Mater.*, 2017, **16**, 363-369.

25. Z. Xiao, X. Jia and L. Ding, *Sci. Bull.*, 2017, **62**, 1562-1564.

26. Y.-C. Lin, H.-W. Cheng, Y.-W. Su, B.-H. Lin, Y.-J. Lu, C.-H. Chen, H.-C. Chen, Y. Yang and K.-H. Wei, *Nano Energy*, 2018, **43**, 138-148.

27. G. Zhang, K. Zhang, Q. Yin, X. F. Jiang, Z. Wang, J. Xin, W. Ma, H. Yan, F. Huang and Y. Cao, *J. Am. Chem. Soc.,* 2017, **139**, 2387-2395.

28. W. Zhao, S. Li, S. Zhang, X. Liu and J. Hou, *Adv. Mater.*, 2017, **29**, 1604059.

29. H. Chen, Z. Hu, H. Wang, L. Liu, P. Chao, J. Qu, A. Liu, W. Chen and F. He, *Joule,* 2018, **2**, 1623-1634.

30. T. Liu, L. Huo, X. Sun, B. Fan, Y. Cai, T. Kim, J. Y. Kim, H. Choi and Y. Sun, *Adv. Energy Mater.,* 2016, **6**,1604059.

31. J. Lee, V. Tamilavan, K. H. Rho, S. Keum, K. H. Park, D. Han, Y. K. Jung, C. Yang, Y. Jin, J.-W. Jang, J. H. Jeong and S. H. Park, *Adv. Energy Mater.,* 2018, **8**, 1702251.

32. W. Li, D. Yan, F. Liu, T. Russell, C. Zhan and J. Yao, Sci. China Chem., 2018, DOI:

10.1007/s11426-018-9320-3.

33. D. Yan, J. Xin, W. Li, S. Liu, H. Wu, W. Ma, J. Yao and C. Zhan, *ACS Appl. Mater. Interfaces*, 2018, DOI: 10.1021/acsami.8b17246.

34. Y. Chen, P. Ye, Z.-G. Zhu, X. Wang, L. Yang, X. Xu, X. Wu, T. Dong, H. Zhang, J. Hou, F. Liu and H. Huang, *Adv. Mater.*, 2017, **29**, 1603154.

35. P. Cheng, C. Yan, Y. Wu, J. Wang, M. Qin, Q. An, J. Cao, L. Huo, F. Zhang, L. Ding, Y. Sun, W. Ma and X. Zhan, *Adv. Mater.*, 2016, **28**, 8021-8028.

36. Z. Wang, X. Zhu, J. Zhang, K. Lu, J. Fang, Y. Zhang, Z. Wang, L. Zhu, W. Ma, Z. Shuai and Z. Wei, *J. Am. Chem. Soc.*, 2018, **140**, 1549-1556.

37. J. Yuan, W. Guo, Y. Xia, M. J. Ford, F. Jin, D. Liu, H. Zhao, O. Inganas, G. C. Bazan and W. Ma, *Nano Energy*, 2017, **35**, 251-262.

38. P. Mueller-Buschbaum, *Adv. Mater.*, 2014, **26**, 7692-7709.

39. Y.-C. Lin, Y.-J. Lu, C.-S. Tsao, A. Saeki, J.-X. Li, C.-H. Chen, H.-C. Wang, H.-C. Chen, D. Meng, K.-H. Wu, Y. Yang and K.-H. Wei, *J. Mater. Chem. A*, 2019, **7**, 3072-3082.

40. J. Rivnay, S. C. Mannsfeld, C. E. Miller, A. Salleo and M. F. Toney, *Chem. Rev*., 2012, **112**, 5488-5519.

41. Z. Hu, H. Chen, J. Qu, X. Zhong, P. Chao, M. Xie, W. Lu, A. Liu, L. Tian, Y. Su, W. Chen and F. He, *ACS Energy Lett.,* 2017, **2**, 753-758.

42. H. Hu, K. Jiang, P. C. Y. Chow, L. Ye, G. Zhang, Z. Li, J. H. Carpenter, H. Ade and H. Yan, *Adv. Energy Mater*., 2018, **8**, 1701674.

43. C. Leow, T. Ohnishi and M. Matsumura, *J. Phys. Chem. C*, 2013, **118**, 71-76.

44. M. T. Sajjad, A. J. Ward, C. Kastner, A. Ruseckas, H. Hoppe and I. D. Samuel, *J. Phys.*

Chem. Lett., 2015, **6**, 3054-3060.

45. A. C. Mayer, S. R. Scully, B. E. Hardin, M. W. Rowell and M. D. McGehee, *Mater. Today*, 2007, **10**, 28-33.
46. M. T. Sajjad, O. Blaszczyk, L. K. Jagadamma, T. J. Roland, M. Chowdhury, A. Ruseckas and I. D. W. Samuel, *J. Mater. Chem. A*, 2018, **6**, 9445-9450.
47. T. Kirchartz, T. Agostinelli, M. Campoy-Quiles, W. Gong and J. Nelson, *J. Phys. Chem. Lett.*, 2012, **3**, 3470-3475.
48. P. P. Khlyabich, A. E. Rudenko, R. A. Street and B. C. Thompson, *ACS Appl. Mater. Interfaces*, 2014, **6**, 9913-9919.

Table of Contents

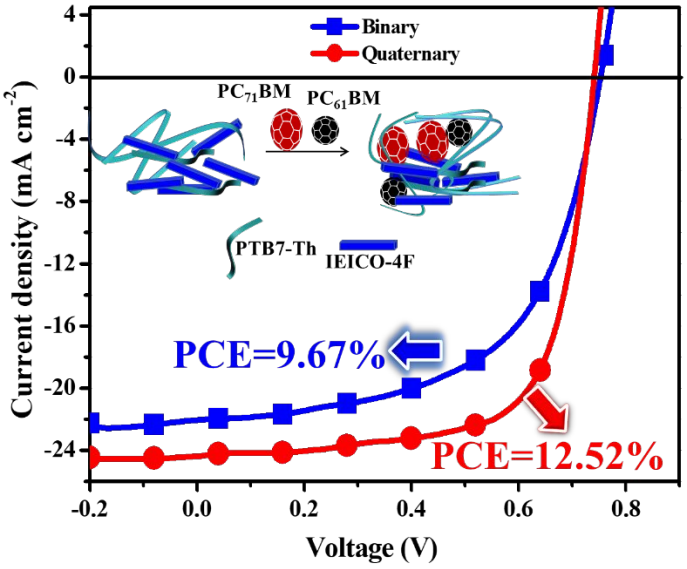

Two typical fullerene derivatives were incorporated PTB7-Th:IEICO-4F binary host to enable an efficient quaternary polymer solar cells with PCE up to 12.52%.